



# Numerical Study for the Effect of Secondary Fluid Inlet Geometrical Parameters on the Performance of Water-Steam Two-Phase Ejector used for Desalination System

Mustafa S. Mahdi<sup>1\*</sup>, Akram W. Ezzat<sup>1,2</sup>

<sup>1</sup>Department of Mechanical Engineering, University of Baghdad, Baghdad 10071, Iraq

<sup>2</sup>School of Mechanical Engineering, The University of Adelaide, Adelaide, SA 5005, Australia

## ARTICLE INFO

### Article history:

Received December 6, 2024

Revised January 29, 2025,

Accepted February 8, 2025

Available online June 1, 2025

### Keywords:

Two-phase ejector

Entrainment ratio

Secondary fluid inlet angles

Multiple secondary fluid inlet streams

## ABSTRACT

This study investigates the effect of secondary fluid inlet geometrical parameters on the performance of a two-phase water-steam ejector operating in the subsonic flow regime. A 3D numerical model, employing the Volume-of-Fluid (VOF) method, was developed to analyze the impact of varying secondary fluid inlet angles (30°, 45°, 60°, 75°, and 90°) and the number of secondary fluid inlets (1, 2, 3, and 4). The study examined these parameters across a range of primary fluid flow rates (6-24 L/min) to understand their interactions. The numerical model was validated through comparison with existing experimental data, demonstrating strong agreement between predicted and measured ejector entrainment ratios (Er). An optimal secondary fluid inlet angle of 45° was identified, providing the best balance between momentum transfer and perpendicular velocity components. It was found also that increasing the number of secondary fluid inlets from 1 to 3 significantly enhanced the ejector Er, while further increases yielded minimal additional improvements. The effects of secondary fluid inlet parameters were more pronounced at higher primary fluid flow rates. These results contribute to a deeper understanding of two-phase ejector performance and provide valuable insights for optimizing their design in various applications.

## 1. Introduction

Ejectors, also known as thermo-compressors, have gained prominence in various engineering applications due to their advantages such as self-starting operation, silent operation, energy efficiency, and the absence of moving parts. These devices are employed in waste heat recovery systems [1], aerospace and ocean navigation [2, 3], food processing [4], desalination [5, 6], refrigeration [7, 8], and hydrogen production [9].

Ejector performance is significantly influenced by the mixing of high-pressure primary fluid with low-pressure secondary

fluid, which is strongly dependent on the ejector's geometry [10]. Understanding this relationship is crucial for designing efficient ejectors.

In flash evaporation systems, two reservoirs are typically employed: a high-pressure reservoir and a low-pressure reservoir to provide the necessary superheated conditions. An ejector can be integrated into such systems to enhance performance by inducing secondary flow. This study focuses on a two-phase ejector using water as the primary fluid and steam as the secondary fluid, a configuration commonly employed in single-stage flash evaporation

\* Corresponding author.

E-mail address: [mustafasmahdi@gmail.com](mailto:mustafasmahdi@gmail.com)

DOI: [10.24237/djes.2025.18208](https://doi.org/10.24237/djes.2025.18208)

This work is licensed under a [Creative Commons Attribution 4.0 International License](https://creativecommons.org/licenses/by/4.0/).



desalination systems [11]. Extensive research has been conducted to gain a deeper understanding of ejector design and operation for various applications; Nakagawa et al. [12] investigated the effects of mixer length on ejector system performance. The ejector employed in CO<sub>2</sub> refrigeration cycle, and the mixer lengths were 5, 15 and 25 mm. The experimental results showed that the mixer length has a significant effect on ejector entrainment ratio  $Er$ , which reaches the minimum value at 5 mm mixer length and the maximum value at 15 mm. The system performance (COP) was improved by 10% due to improved mixer size. Yan et al. [13] conduct a numerical study with experimental validation to investigate the effect of six different geometrical parameters (area ratio, primary nozzle exist position, mixer length, primary nozzle diameter, angle of constant-pressure mixing section and the diameter of constant-area mixing section) on the performance of the ejector  $Er$  for an air-cooled ejector cooling system. The study found that the area ratio and the nozzle outlet location are significant parameters affecting on the ejector  $Er$ . A new ejector was designed according the optimal parameters found in the numerical results and applied at the same cooling system. It found that a significant performance improvement was achieved by using the new ejector design. Cui et al. [14] performed a numerical study for gas–gas ejectors and gas–liquid ejectors at supersonic flow to evaluate  $Er$  behaviour; this study was experimentally validated. The numerical results showed that the shock wavelength has a dominant effect on the  $Er$  of the ejector. A clear difference is observed in shock length for gas–gas and gas–liquid ejectors, due to the viscosity difference of the operating fluids within the range of 0.01–1.0. The optimal length of mixing chamber to diameter ratio found is about 1–2 for gas–liquid ejectors and 5–7 for gas–gas ejectors. Ping et al. [15] performed a numerical study of a two-phase ejector in transient mode to determine the optimal operation condition for high-performance ejector. The considered working fluids are Liquefied-Natural-Gas as primary fluid and Boiling-Off-Gas as secondary fluid and the investigated operation conditions

are axial velocity, pressure and temperature. The result found that the  $Er$  increased with increasing primary fluid flow rate and decreasing outlet pressure. The optimal ejection  $Er$  was found when the Liquefied-Natural-Gas velocity inlet equal to 11–12 m/s, Boiling-Off-Gas pressure of 0.101–0.507 MPa and ejector outlet pressure of 0.101–0.304 MPa. Whendig et al. [5] numerically investigate a variable geometry of ejector (auto-tuning area ratio (AR) ejector) to enhance the performance of multiple effects desalination with vapor compression (MED-TVC) desalination system. The CFD model was validated experimentally for confidently study the AR effect on the ejector performance. A correlation to estimate the optimal area ratio for different primary and back pressure was developed. The results show that the auto-tuning ejector could achieve a high entrainment ratio ( $Er$ ) under different flow conditions and thus a high MED performance could be achieved. When the steam pressure fluctuates from (800–2000) kPa, the average AR ejector  $Er$  is 1.39, higher than the standard ejector (fixed geometry ejector) of 0.69 with a critical back pressure of 20 kPa. Jiapeng et al. [6] established a mathematical model built on real gas theory to study the effect of condensation degree, entropy generation and exergy destruction on the steam ejector performance employed in desalination applications. The study found that condensation is a general occurrence in the ejector parts. It was found also that all the condensate liquid droplets at the choking part could be evaporated by increasing the superheat degree of the inlet steam to 35 K. The results show that the mixing process irreversible loss is 73% of the total irreversible losses of the ejector if the steam is at the saturation condition. Xuhui et al. [16] performed a 2D numerical study for an ejector applied to a 80 kW polymer electrolyte membrane fuel cell system and determined the effects of mixer diameter, diffuser angle and humidity of the secondary fluid on the ejector performance. The numerical results showed that the optimal diffuser angle is between 11° to 13°, at which the ejector exhibits the best performance. It was found also that the mixer diameter and the secondary fluid humidity

significantly affect the ejector Er. Han et al. [17] numerically studied the separation of boundary layer, the reason behind the separation, the separated region location and the boundary layer separation effect on steam ejector Er applied in refrigeration system. The results show that in a particular size of the throat diameter and nozzle exit positions, the ejector worked in critical mode and has an optimal performance when the other conditions were constant. In the case of varying the throat diameter or a large nozzle exit positions, the separation of the boundary layer became significant and the mixed fluid couldn't overcome the back pressure to exit from the ejector and the ejector efficiency descended to zero. The study showed that the ejector geometry is an important factor that influences the degree of boundary layer separation. Akram et al. [18] performed an experimental and theoretical study to investigate the steam ejector ability to induce a secondary flow under different operation conditions. The ejector connected to a desalination system which where integrated by a solar collector. The experiment conditions were: the primary steam inlet temperature and pressure are: (106-107) °C while the condenser pressure range is (0.974-1) bar. It was found that the system productivity of distilled water increased by 5.5 % due to using the ejector, and the analysis shown that 34% of the thermal energy required for the system to complete the desalination process was covered by the solar energy collector. Shaker et al. [8] perform a numerical simulation to investigate the effect of geometrical and operation condition of steam ejector performance. The results show that if the nozzle throat diameter increased from 2.4 to 2.8 mm the Er decreases by 40% at a boiler temperature of 120°C, also by increasing the evaporator temperature from 7.5 to 15 °C the Er increased by 65.57%. the results show also that if the second shock series position is close to the diffuser the ejector runs in critical mode. In contrast, if its position moves toward the upstream, the ejector runs in subcritical mode so the second shock series position effect the ejector operation mode. Egoi [19] proposed a new variable mixing chamber ejector to overcome the inflexibility of the waste heat used for chiller operation. The study was

performed using a computational fluid dynamic (CFD) model and compared with experimental data from literature. The study found that the modification of the proposed mixing chamber gives an increase in the cooling capacity of the chiller without supplying more energy. The proposed design enhances the cooling capacity up to 120% at low condensation temperatures and a reducing of 8 °C of the critical temperature. It means that by using the proposed ejector the system that works at 33 °C now it could operate at 41 °C

Yan et al. [20] conduct a 3-D numerical study to optimize the ejector cross section area and the secondary flow inlet angle. The model studied also the auxiliary entrainment effect on the ejector Er. The numerical results show that the perpendicular direction of the secondary flow to the primary flow is a little better than the parallel flow direction. Also, it was found that the cross-section area of the secondary flow has an effect on the entertainment ratio but this effect is vanished when the area increased to a certain value. The results show also that auxiliary entrainment inlet are vital parameter affecting the ejector Er. Finally, it was shown that after optimization of geometry parameters and auxiliary entrainment inlet, the ejector Er can be enhanced by 97.7%. Yao et al. [21] performed a 3D numerical study of high pressure steam water condensing ejector based on inhomogeneous multi-phase model. The study investigates the changes in steam plume shape, the thermal hydraulic parameter distribution and pressure relation under different boundary conditions: of steam inlet pressure range of (0.7-2.4) MPa and mass flow rate of (1019-3310) kg/ (m<sup>2</sup> s) MPa. The results show that the increase of steam inlet mass flow rate and decrease of back pressure transform the steam plume shape from ellipsoidal to divergent shape where the choking phenomenon is observed. Jingyang et al. [22] perform a numerical study with experimental validation to investigate the influence of mixer and diffuser diameter on the Er of an ejector used in an aeroengine air system. The numerical results showed that when the compression ratio is 1.17 and the mixer diameter increase from 3 mm to 9 mm the enhancement in ejector Er is 23.1%. The

maximum achieved in ejector  $Er$  is 211 % at mixer diameter of 27 mm. It was found that when the ejector size is very small, a strong shock wave could suppress the primary and the secondary fluids mixing, and thereby causes an increase in the total ejector loss. Meiqi et al. [23] Numerically Studied the effect of primary nozzle throat blocking area ratio and the dryness fraction at the primary and the secondary fluid on the two-phase ejector performance. The study found that the ejector performance is decreasing with the decreasing of primary fluid dryness fraction and increasing with the decreasing of secondary fluid dryness fraction. It was found that the ejector  $Er$  is improved by 253.3% at dryness fraction of 1 and 0.4 of primary and secondary fluid respectively. Also the study found an optimal value for the blockage area ratio. It was concluded that regardless the varying of area ratio or the dryness fraction the adjustment of ejector operation condition could enhance the performance of the ejector. Omar et al. [24] Numerically studied the effect of different ejector geometrical parameter focusing and on the area ratio of the ejector. The ejector is employed in ammonia solar cooling system. The effect of primary and secondary fluids temperatures on the ejector  $Er$  were investigated also. The numerical model considers  $k-\epsilon$  model to simulate flow turbulence and the model was experimentally validated. The study found that at primary fluid temperature of 90 °C and secondary fluid temperature of 15 °C the optimal ejector area ratio was 6.44 at which the COP of the cooling system was 0.547. The study presents a pre-experimental design and providing more insight to the flow phenomena inside the ejector. Xinyuan et al. [25] Perform a numerical study for a hydrogen ejector employed in proton exchange membrane fuel cell. The model considers a pulse flow for the gas by user define function, to study the pulse flow effects on the ejector  $Er$  and compare it with the ejector  $Er$  for steady flow case. The study found that the pulse flow enhances the ejector  $Er$  compared to the steady flow under a variable range of primary fluid flow rate. It was found that maximum steady flow ejector  $Er$  was 3.2 while it was 3.5 for the pulse flow ejector

under the same condition i.e. the ejector  $Er$  enhanced by 9.8% due to the pulse flow. The effect of pulse flow was more pronounced at low pressure working that the ejector  $Er$  increase by 16.6%. finally, the gas pulse flow was compared under different frequencies and it was found that at 1 Hz the pulse flow exhibits the best ejector performance. Hamid et al. [26] Study the effect of primary flow temperature on the ejector performance, the ejector employed in a power plant condenser to remove air by creating vacuum. The study considers other parameters such entropy generation, steam production and air suction cost. The studied primary flow temperatures were in the range of 350 °C to 400 °C which is the operation range of the power plant condenser. The results show that the increasing of primary fluid temperature enhances the ejector  $Er$  and decrease the steam production and air suction cost. For example, by increasing the primary fluid temperature from 350 °C to 400 °C the air suction cost reduced by 2%. Xianying et al. [27] Numerically analysis the performance of vertical layout ejector employed for gas air mixing in infrared stove. The numerical model was validated with an experimental ejector test rig. The study investigates the effect of mixing tube length and diameter on the ejector  $Er$  also. The numerical results show that the increasing the mixer tube length decrease the combustion excess air coefficient. The maximum ejector performance at which the excess air coefficient is at peak values of 1.13 the mixer diameters values were equal to 9.8 mm, 11.2 mm, and 12.6 mm at 3.5°, 4.7°, and 5.0°, respectively.

A review of existing literature reveals that most studies have focused on the impact of nozzle, mixer, and diffuser geometry on ejector performance ( $Er$ ). However, there is a dearth of research investigating the effects of secondary fluid flow direction and, more specifically, the division of the secondary fluid inlet into multiple streams. The study examined these parameters across a range of primary fluid flow rates to understand their interactions. The study aimed to enhance the ejector  $Er$  in term of the considered parameters to increase the secondary fluid (steam) flow rate thereby increase the fresh water production. This leads to lower operation

cost and contribution to sustainable desalination system. This study addresses these knowledge gaps by exploring the influence of these novel parameters on ejector performance. A 3D numerical simulation for the flow in the ejector would be performed using a CFD model and the predicted result would be compared with experimental data from the literature.

## 2. Physical model

To investigate the influence of secondary fluid inlet angle and the number of secondary fluid streams on ejector performance ( $E_r$ ), five models were constructed with varying secondary fluid inlet angles of  $30^\circ$ ,  $45^\circ$ ,  $60^\circ$ ,  $75^\circ$ , and  $90^\circ$  (Figure 1). Additionally, four models with different numbers of secondary fluid inlets (1, 2, 3, and 4) were developed at inlet angle of  $45^\circ$  (Figure 2). The increasing of

secondary fluid inlet stream was while maintaining the total cross section area of the secondary fluid inlets constant and equal to  $0.000154 \text{ m}^2$ , to allow a fair comparison for the ejector performance between the studied cases. The ejector geometry, as detailed in Table 1 and Figure 3, was maintained constant throughout the study, except for the variations in secondary fluid inlet angle and number of inlets explained in Figures 1 and 2. The primary fluid was liquid water (under variable range of flow rates (6-24 L/min) to understand their interactions with the studied parameters), while the secondary fluid was steam. These primary fluid flow rates values were considered to encompass the typical and maximum flow rate of the operating condition of evacuated tube solar collector [28] that integrated with the flash evaporation desalination system for preheating of the saline water

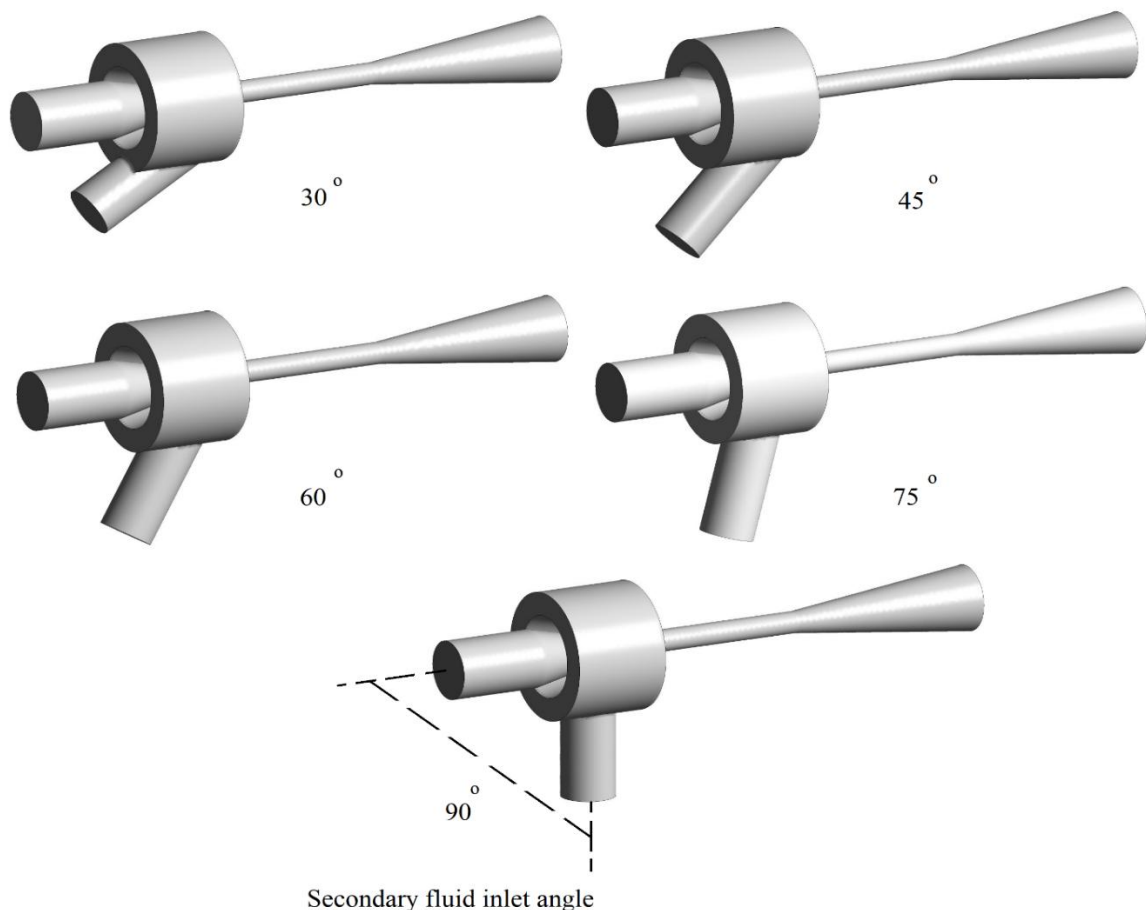


**Figure 1.** Computational domains of the studied ejector with different secondary fluid inlet angles of  $30^\circ$ ,  $45^\circ$ ,  $60^\circ$ ,  $75^\circ$ , and  $90^\circ$ .

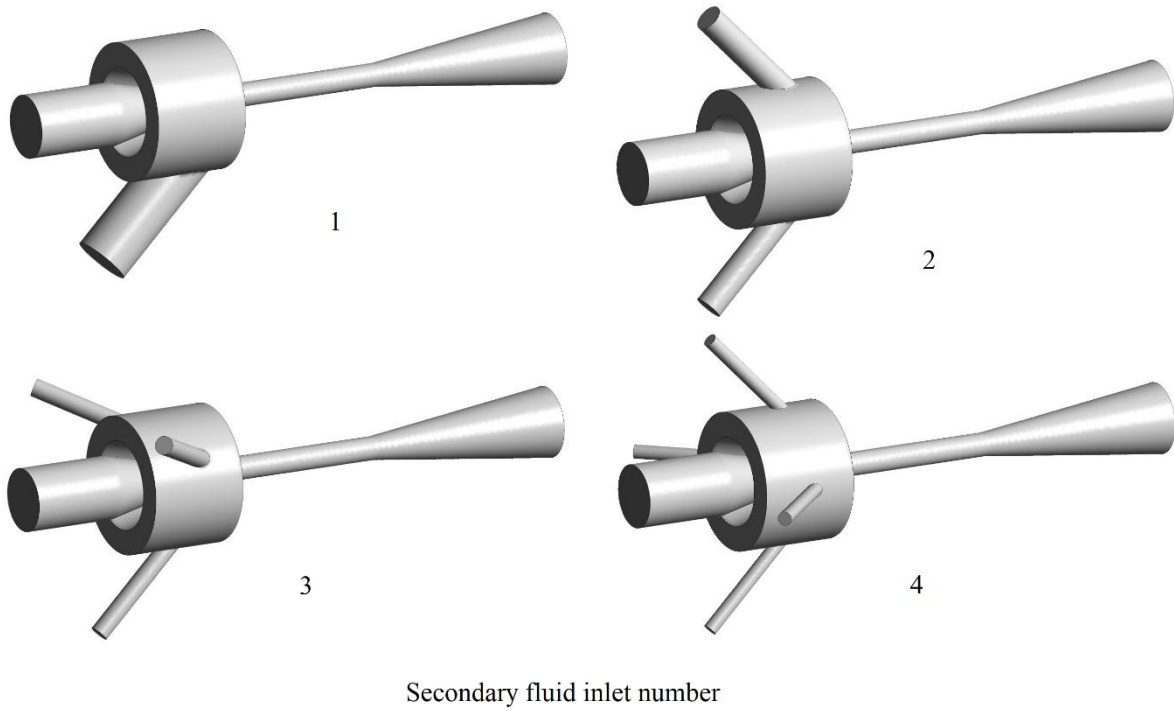


**Figure 2.** Computational domains of the studied ejector with different secondary fluid inlet inlets number (1, 2, 3, and 4).

**Table 1** Ejector geometric dimensions.

Geometry (refer to figure 3)	Value
Primary fluid inlet diameter	26.7 (mm)
Secondary fluid inlet diameter	21.3 (mm)
Diffuser outlet diameter	26.7 (mm)
Nozzle outlet diameter	1.5 (mm)
Mixer diameter	6 (mm)
Mixer length	40 (mm)
Diffuser angle	6°
Diffuser length	50 (mm)
Ejector material	Plexiglas

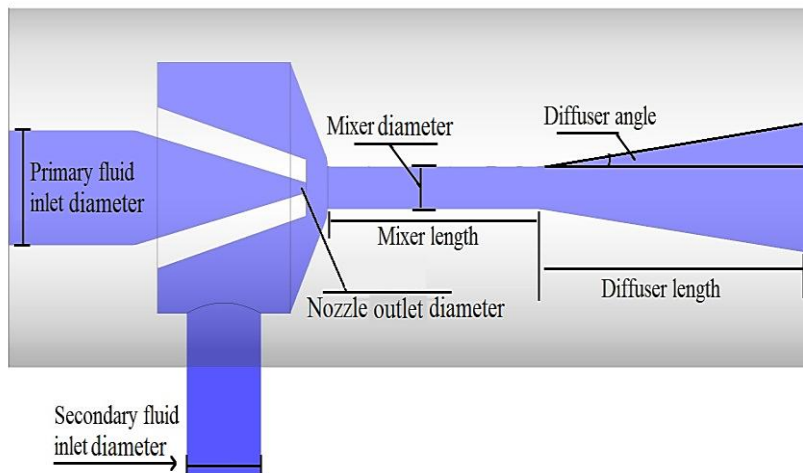


**Figure 3.** The visual representation of ejector geometry mentioned in table 1.

### 3. Numerical model

#### 3.1. Governing equations

A 3D numerical model was developed to investigate the effect of secondary flow inlet geometric parameters on a two-phase ejector's performance which it is essential to accurately capture the complex flow patterns within the ejector, particularly the swirling flow and potential recirculation zones that arise due to the interaction of the primary and secondary fluid streams. The model, depicted in Figure 1 and 2, employed the Volume of Fluid (VOF) method [29, 30], renowned for its accuracy in capturing multiphase flow dynamics [30]. The VOF model ensured mass conservation and accurately represented the heat and mass transfer between the primary (water) and secondary (steam) fluids during the evaporation process. A standard turbulence model  $k_\omega$ , validated through comparisons with experimental data for two-phase ejectors [15, 17], was adopted to capture the complex flow characteristics. The model is steady state and its governing equations (1-7) for this model are presented below [30]:

$$\nabla \cdot (\alpha_l \vec{v}) = \frac{S_M}{\rho_l} \quad (1)$$

$$\nabla \cdot (\alpha_v \vec{v}) = \frac{S_M}{\rho_v} \quad (2)$$

The momentum equation is:

$$\nabla \cdot (\rho \vec{v} \vec{v}) = -\nabla P + \nabla \cdot [\mu (\nabla \vec{v} + \nabla \vec{v}^t)] + \rho \vec{g} + F_i \quad (3)$$

The energy equation is:

$$\nabla \cdot (\rho \vec{v} h) = \nabla \cdot (k \nabla T) + S_E \quad (4)$$

In the VOF model, enthalpy ( $h$ ) and temperature are taken as average quality variable:

$$h = \frac{\alpha_l \rho_l h_l + \alpha_v \rho_v h_v}{\alpha_l \rho_l + \alpha_v \rho_v} \quad (5)$$

The volume fraction equation is solved for vapour phase only and as the following:

$$\nabla \cdot (\alpha_v \rho_v \vec{v}) = S_M \quad (6)$$

$$\alpha_v + \alpha_l = 1 \quad (7)$$

The total cell volume comprises vapor and liquid volumes. The liquid volume fraction is calculated using the equation 7.

where

$S_M$  Is the mass source term employed to model mass transfer during the evaporation process.

$F_i$  is the interphase forces.

$S_E$  is the energy source term used to estimate the heat transfer during evaporation process.

In the above equations,  $\rho$ ,  $\alpha$ ,  $\vec{v}$ ,  $P$ ,  $\mu$ ,  $g$ ,  $k$  and  $T$  are the density, volume fraction, velocity vector, pressure, the dynamic viscosity, the gravity acceleration, thermal conductivity and temperature, respectively.

#### 3.2. Boundary conditions

- Primary Fluid: A velocity inlet was specified for the primary fluid (liquid water) due to its negligible compressibility [15]. Inlet velocities of 0.5, 1, and 2 m/s were considered to maintain subsonic flow (Mach number < 0.3). The assumption of subsonic flow is considered in this work as the ejector works with liquid (water) as a primary fluid and applied in a desalination system utilizes a flat plate solar water heater, which typically provides a limited flow rate of heated brine.
- Secondary Fluid: A pressure inlet was specified for the secondary fluid (steam) with a value of -72000 Pa (absolute pressure: 29325 Pa).
- Ejector Outlet: A pressure mixture outlet was defined with a value of -80000 Pa (absolute pressure: 21325 Pa).
- The secondary fluid inlet pressure and the ejector back pressure values were selected to match the operational conditions of available data from similar work [11]
- Turbulent Intensity: Turbulent intensity ( $I$ ) was calculated based on the Reynolds number ( $Re$ ) for all inlets and outlets using the following equation of  $I = 0.16 Re^{-0.125}$  [30].
- Fluid Properties: The primary and secondary fluids were assumed to have constant properties at the specified temperature of 80°C.

#### 3.3. Numerical approach

Numerical simulations were conducted using Ansys Fluent 19 R3 to solve the governing equations. The third-order MUSCL scheme was

employed for energy and momentum equations, while the PRESTO scheme was used for pressure. The modified HRIC method was adopted for volume fraction estimation [30]. A coupled algorithm ensured the convergence of pressure and velocity coupling. Under-relaxation factors of 0.5, 0.5, 0.5, and 0.75 were applied to momentum, pressure, volume fraction, and energy, respectively, to maintain numerical stability. Convergence criteria were established for the continuity, momentum, and energy equations with values of  $1 \times 10^{-5}$  for the continuity and momentum equations and  $1 \times 10^{-6}$  for the energy equation. A grid independence study was conducted, focusing on the  $y^+$  value, a dimensionless parameter crucial for the standard  $k-\omega$  turbulence model. Various grid with different element numbers were generated. The  $y^+$  value was evaluated for each grid, and the process was repeated until a satisfactory value was achieved. For each ejector model four grid configurations with approximately 400,000, 900,000, 2,000,000, and 3,900,000 elements were evaluated to have a grid independence solution. Figure 4

illustrates the variation of  $y^+$  and ejector performance ( $Er$ ) with grid elements number. The  $y^+$  value decreased from approximately 112 at 400,000 elements to 22 at 2 and 3.9 million elements, falling within the acceptable range [31]. Grid independence was achieved with approximately 2 million grid elements, beyond which  $Er$  remained nearly constant at 0.013. This grid density was selected for subsequent simulations to balance computational efficiency and solution accuracy. To enhance grid quality and reduce the number of elements, the tetrahedral grid element was converted to a polyhedral element using the Fluent software (figure 5). This resulted in a grid with approximately 1 million numbers (reduced from 2 million) and an improved element quality of 0.95 (from 0.81). The mesh element and node numbers for each of the considered model geometries are presents in Table 2. The numerical simulations were conducted on a workstation equipped with an Intel Core i7 processor and 16 GB of RAM. The computational time for each simulation was approximately 17 hours.

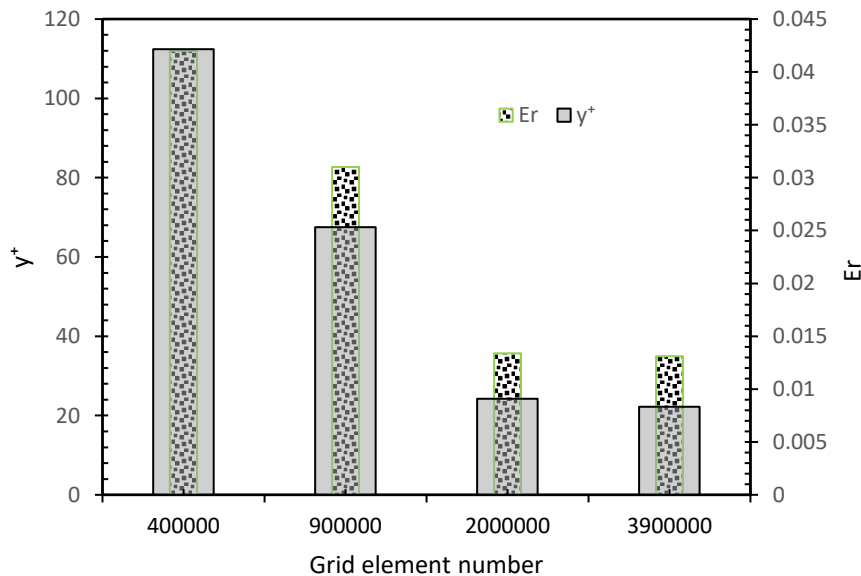


**Figure 4.** The results of a grid independence study and the corresponding  $y^+$  values.

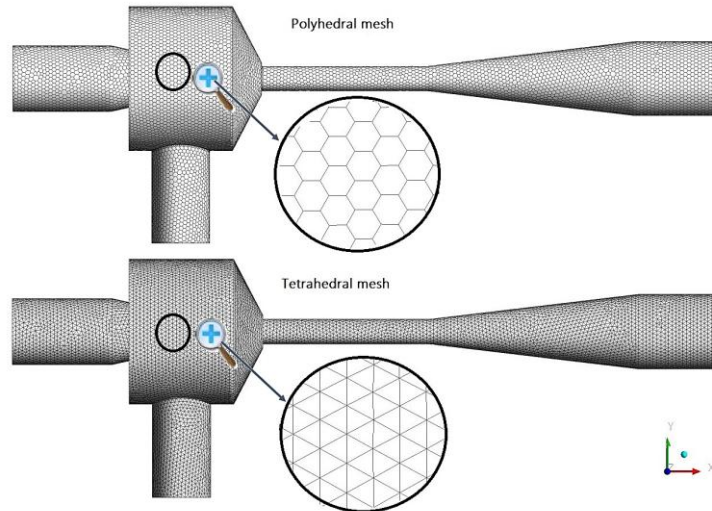


**Figure 5.** Comparison of Polyhedral and Tetrahedral grid elements for the ejector model.

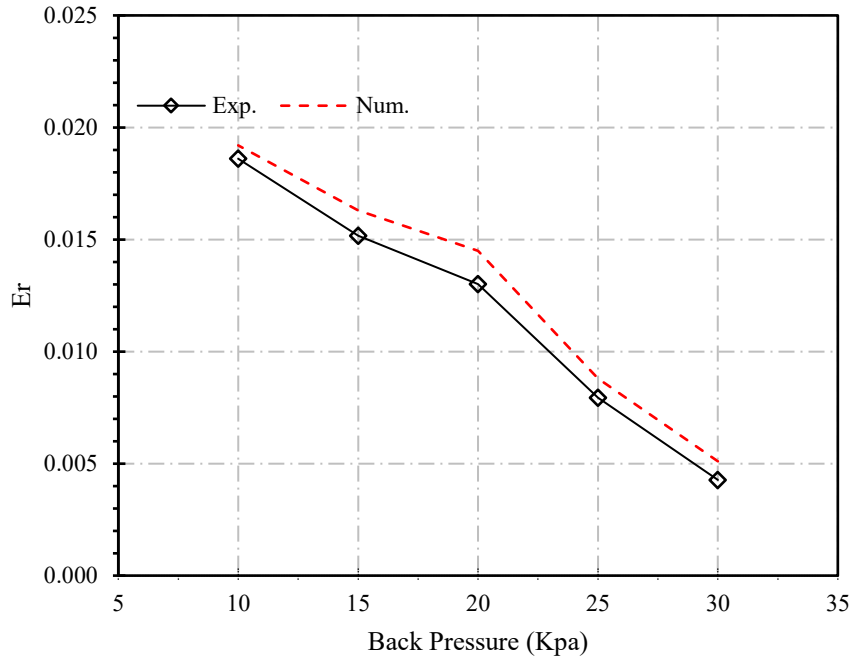
**Table 2:** Mesh statistics for the model geometries.

Geometry	Elements number	Nodes number
30° secondary fluid inlet angles	973,534	6,084,580
45° secondary fluid inlet angles	974,345	6,090,870
60° secondary fluid inlet angles	974,565	6,091,030
75° secondary fluid inlet angles	974,622	6,092,210
90° secondary fluid inlet angles	975,004	6,093,750
1 secondary fluid inlets	974,345	6,090,870
2 secondary fluid inlets	1,010,325	6,312,500
3 secondary fluid inlets	1,019,476	6,368,750
4 secondary fluid inlets	1,032,454	6,450,000

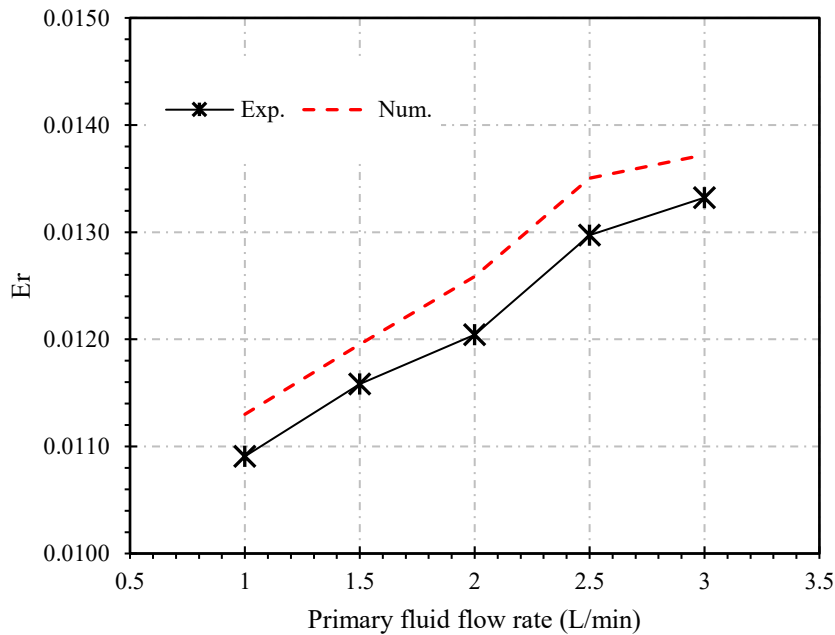
### 3.4. Numerical model validation

A comprehensive validation of the numerical model was conducted against existing experimental data for two-phase ejectors. The experimental ejector employed in a single-stage flash evaporation desalination system, utilized water as the primary fluid and steam as the secondary fluid [11]. Experiments were conducted with primary fluid flow rates ranging from 1 to 3 L/min, a primary fluid temperature and pressure of 80°C and 101 kPa, respectively, and a secondary fluid temperature and pressure of 80°C and 29,000 kPa, respectively. The back pressure was varied from 10 to 30 kPa. The experimental ejector's dimensions matched those of the numerical model, as detailed in Table 1. Both qualitative and quantitative comparisons were performed between experimental measurements and numerical results to assess the model's ability to accurately capture the complex two-phase flow dynamics within the ejector.

Figure 6-a presents a comparison of experimental [11] and numerical ejector performance ( $Er$ ) across varying back pressures. Both experimental measurements and numerical results of  $Er$  show the same curve trend that they are decreasing with the increasing of back pressure values. Figure 6-b presents a comparison of experimental [11] and numerical ejector performance ( $Er$ ) across varying primary fluid flow rates. Also, both experimental and numerical results demonstrate an increase in  $Er$  with rising primary fluid flow rate. While the numerical model consistently predicted slightly higher  $Er$  values compared to experimental data (average difference of 4.1%), this discrepancy can be attributed to the complexity of turbulence phenomena. The standard turbulence model may not have fully captured the energy dissipation occurring at the ejector walls. Nonetheless, the difference between experimental and numerical  $Er$  values remained within an acceptable range of 5% [21].



a)



b)

**Figure 6.** comparison of experimental and numerical  $Er$  at (a) at different primary fluid flow rates, (b) at different back pressures.

A qualitative validation was conducted by comparing the flow visualization of the experimental ejector image [11] with the numerical model's velocity streamlines and liquid fraction contour (Figure 7). Both experimental and numerical results demonstrated similar flow patterns, with a slight tendency towards the top side of the ejector

diffuser due to reverse flow at the lower diffuser wall. This phenomenon can be attributed to flow separation at the diffuser's diverging wall. The alignment between experimental and numerical observations confirms the model's ability to accurately capture the complex two-phase flow dynamics within the ejector.

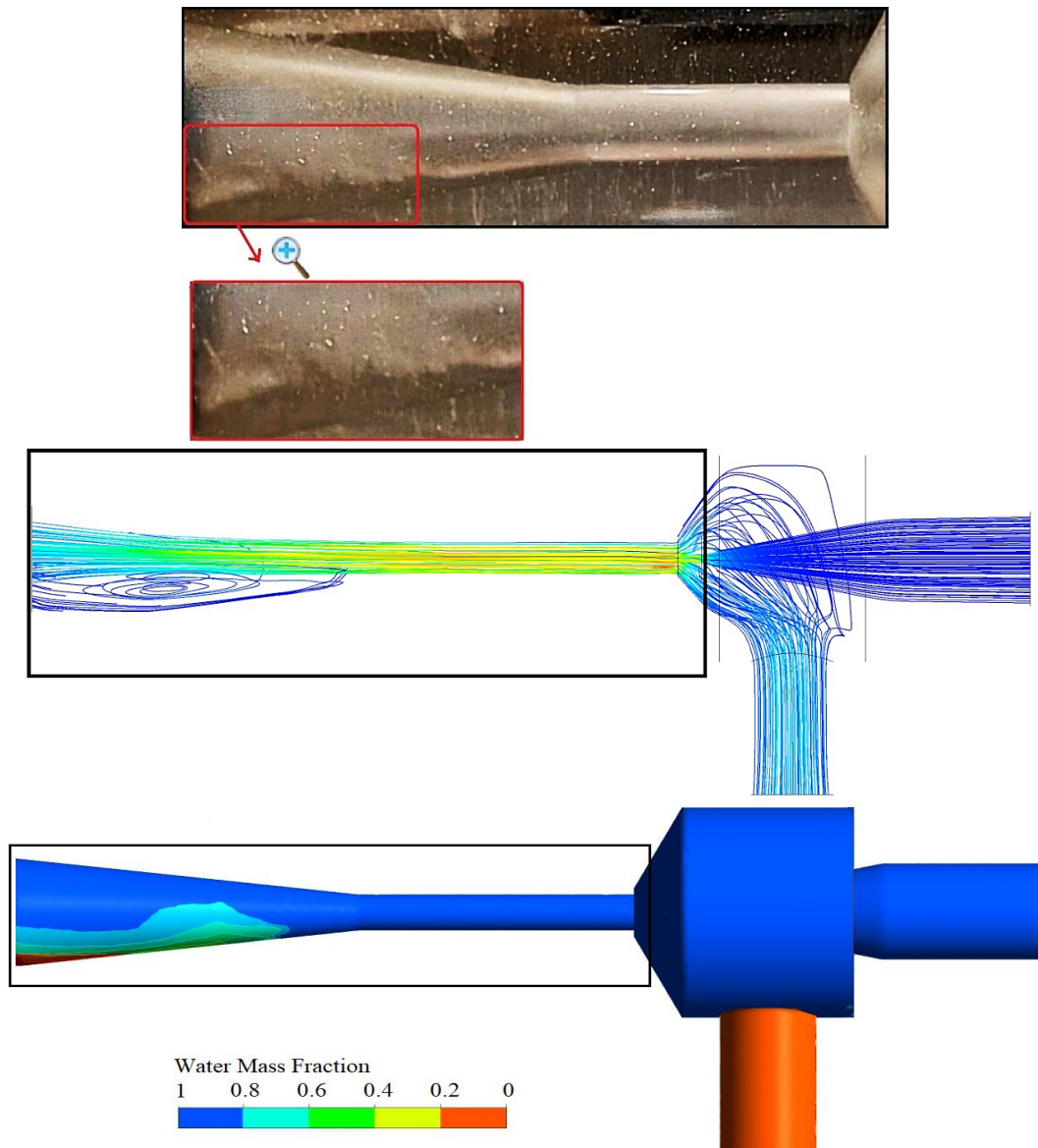


Figure 7. Comparison of real flow image with flow velocity streamline of the numerical model

#### 4. Results and discussion

The variation effect of the secondary fluid inlet angle on a two-phase ejector performance ( $E_r$ ) is presenting in figure 8. The studied secondary fluid inlet angles are  $30^\circ$ ,  $45^\circ$ ,  $60^\circ$ ,  $75^\circ$  and  $90^\circ$ , each angle where investigated under three primary fluid inlets of 6, 12 and 24 L/min while the other operation and design condition are constant and as mentioned in physical and boundary condition sections. It could be seen from the figure that the  $45^\circ$  secondary fluid inlet provide the best ejector performance ( $E_r$ ), while the  $60^\circ$ ,  $75^\circ$  and  $90^\circ$  inlet angle have almost similar ejector  $E_r$  and lower to that of  $45^\circ$ . The  $30^\circ$  secondary inlet

angle have the lowest ejector  $E_r$ . This behavior is clear at the primary fluid flow rate of 12 and 24 L/min and almost vanished at low flow rate of 6 L/min i.e. the effects of secondary fluid inlet angle is disappearing at low primary fluid flow rate. Figure 8 also shows that the ejector  $E_r$  is increasing significantly by increasing the primary fluid flow rate from 6 to 24 L/min. The explanation for the optimal secondary fluid inlet of  $45^\circ$  is that this angle provides the optimal balance between the momentum transfer from the primary fluid to the secondary fluid and the secondary fluid velocity component perpendicular to the primary fluid flow. As the inlet angle increases to  $60^\circ$ ,  $75^\circ$ , and  $90^\circ$ , the component of the secondary fluid velocity

parallel to the primary flow increases. This can lead to interaction with less effectively between the primary fluid jet and the secondary fluid, potentially leading to flow separation or recirculation within the mixing chamber. The shallower angle of  $30^\circ$  has the less mixing between the primary and the secondary fluids. This finding agreed with [32] which was attributed to the smoother flow through the inlet passage of  $45^\circ$ . And that is due to the fact that the secondary fluids velocity component which it is perpendicular to the primary fluid flow is a critical factor to determine the ejector

performance of the two-phase flow ejector, a well-balanced combination of parallel and perpendicular velocity component can optimize the momentum transfer and thereby the ejector Er. Decreasing the primary fluid flow rate reduces momentum transfer, making it challenging to overcome wall shear losses and the variations in secondary inlet angle won't be significant effect. As a result, overall ejector performance (Er) is lower at lower flow rates, as the case of primary fluid flow rate 6 L/min compared with that of 12 and 24 L/min.

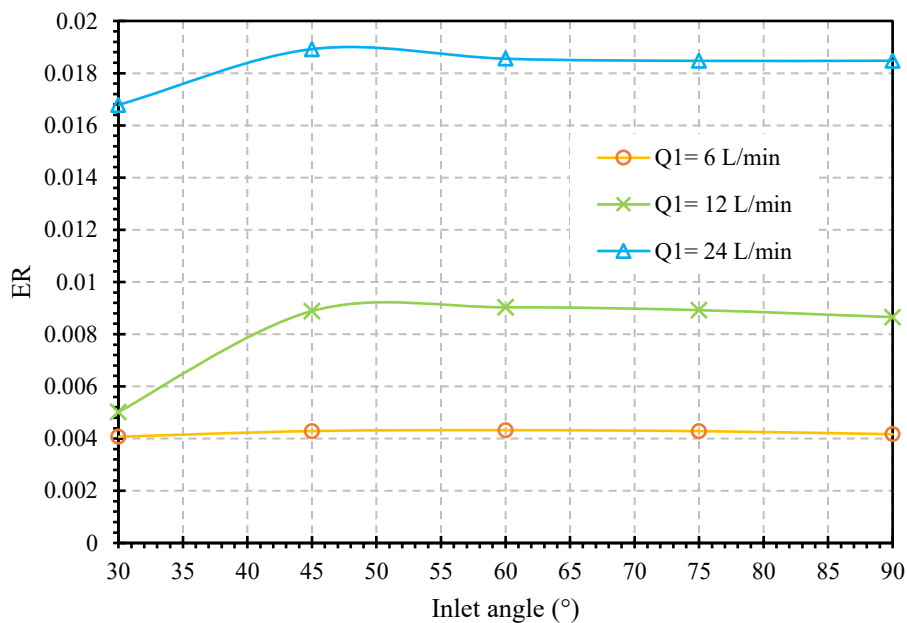
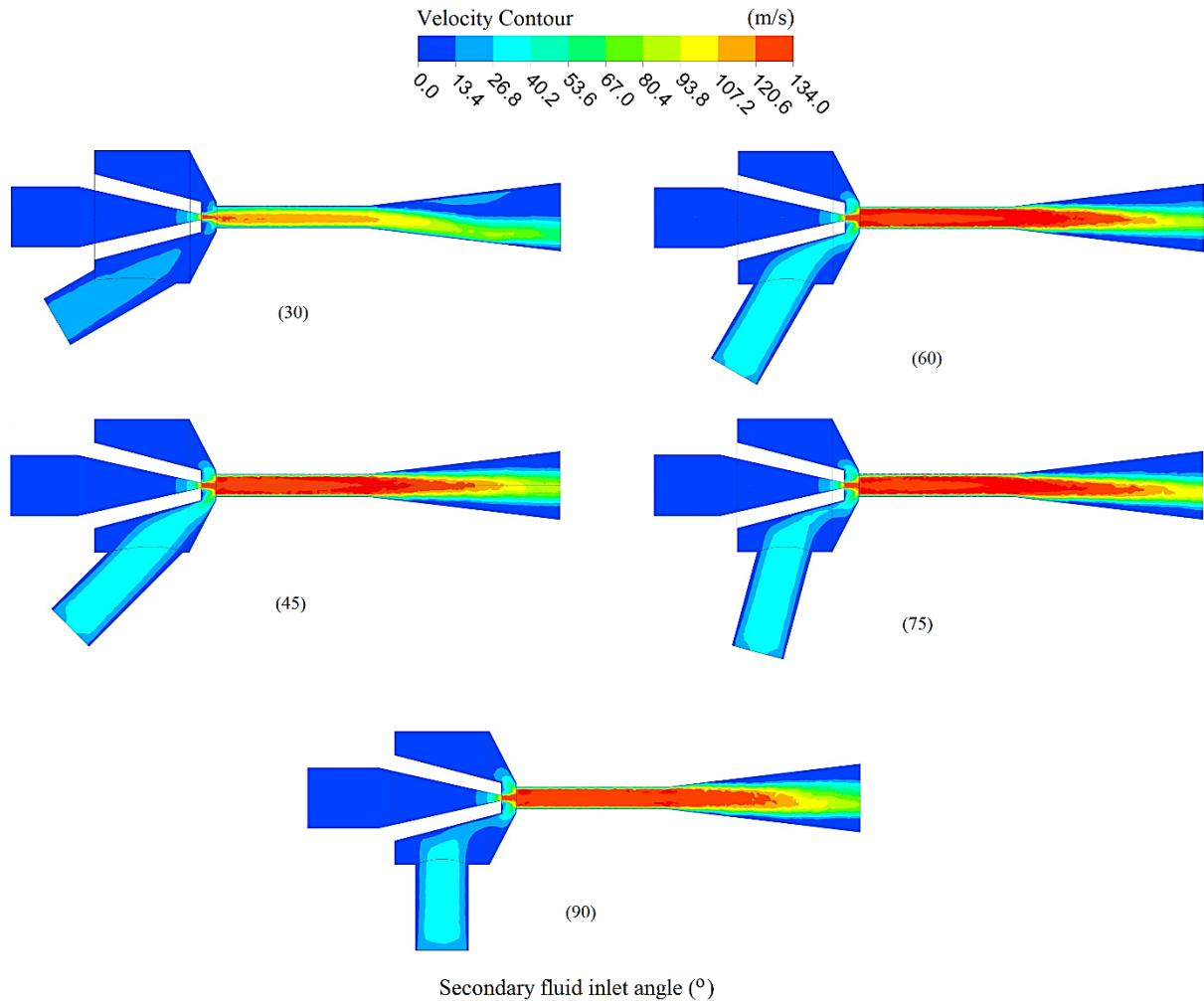


Figure 8. Secondary fluid inlet angle vs ejector Er

The velocity contour for the cases of  $30^\circ$ ,  $45^\circ$ ,  $60^\circ$ ,  $75^\circ$  and  $90^\circ$  secondary fluid inlet angle is shown in Figure 9. The velocity contour is visualized at the ejector mid plane with a velocity range from 0 m/s (blue color) to maximum velocity of red color. And as shown in the legend of Figure 9. The cases of Figure 9 were at 12 L/min primary fluid flow rate and the other operation and design condition are constant and as Figure 8. The figure shows the velocity at the mixer varies from minimum (blue colour) at the mixer wall due to no-slip condition, and the developed velocity boundary layer to maximum (dark red colour) at the adjacent layer then slightly reduces at the centre (light red colour). Figure 9 shows that the

secondary fluids velocity inlet is highest for the case of  $45^\circ$  secondary fluid inlet angle and less for the cases of  $60^\circ$ ,  $75^\circ$  and  $90^\circ$  inlet angle. And the velocity is lowest for the case of  $30^\circ$  secondary fluid inlet angle. The higher the secondary fluid inlet velocity means the higher secondary fluid mass flow rate inlet to the ejector and thereby the higher the ejector Er, and this is agreed with the 12 L/min curve behavior of Figure 8. Figure 9 also shows that the case of  $30^\circ$  inlet angle have a non-uniform flow distribution due to the inefficient mixing and due to the turbulence flow of this case, comparing to the  $45^\circ$  inlet angle which shows the most uniform flow as the flow field converge towards a uniform distribution.



**Figure 9.** Velocity contours of the two-phase ejector at different secondary fluid inlet angle and at primary fluid flow rate of 12 L/min.

To have more insight to the flow behavior under the variation of secondary fluid inlet angle a streamlines visualization is performed and presented in Figure 10 for the same cases and conditions of Figure 9. Figure 10 shows that the case of 45° secondary fluid inlet angle have the most uniform flow for the secondary fluids flow when entering the ejector towards the mixing chamber, the flow is almost ideal with no circulation and turbulence. This behavior leads to the better acceleration to the secondary fluid

and thus the higher Er. This fact could provide another explanation for the superior performance of 45° secondary fluid inlet ejector case. The 30° secondary fluid inlet ejector shows the most fluid flow circulation of the secondary fluids before entering the mixer and confirm the velocity contour of Figure 9 for the non-uniform flow at the ejector. The cases of 60°, 75° and 90° also shows a secondary fluid flow circulation at the inlet but with less intense compared to that of 30° inlet angle case.

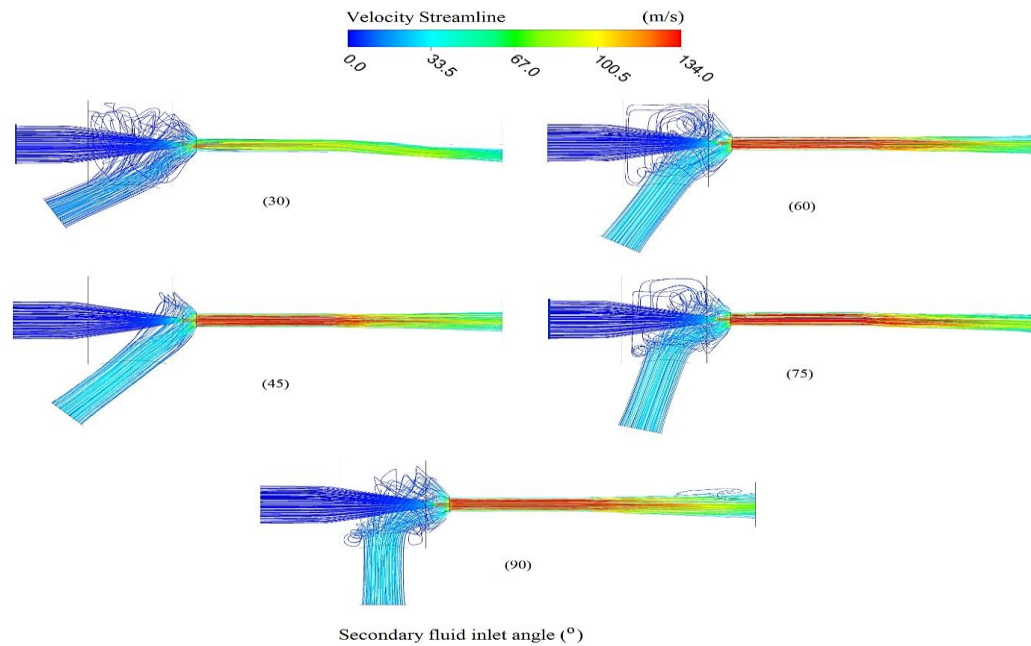


**Figure 10.** Velocity streamlines of the two-phase ejector at different secondary fluid inlet angle and at primary fluid flow rate of 12 L/min.

Figure 11 presents the results of investigating the effect of multiple secondary fluid inlets on the performance ( $Er$ ) of a two-phase water-steam ejector. The considered secondary fluid inlet number for the ejector are 1, 2, 3 and 4 inlets. This increasing was while maintaining the total cross section area of the secondary fluid inlets constant and equal to  $0.000154 \text{ m}^2$ , to allow a fair comparison for the ejector performance between the studied cases. The considered secondary fluid inlet angle is  $45^\circ$  for all the cases as it's the optimal angle that gives the best ejector performance and as explained in the discussion of Figure 8, 9 and 10. Each case of multiple secondary fluid inlet where investigated at three primary fluid flow rate values of 6, 12 and 24 L/min while keeping the other operation and design condition fixed. Figure 11 shows that the ejector  $Er$  is increasing steeply by increasing the secondary fluid inlet from 1 to 3 and this increasing becomes more obvious when increasing the primary fluid inlet from 6 to 24 L/min. The figure also shows that there is no significant enhancement in ejector  $Er$  by increasing the secondary fluid inlet from 3 to 4 at all the examined primary fluid flow rate. The observed enhancement in ejector performance ( $Er$ ) due to increasing of secondary fluid inlets could be due to several reasons; it

can effectively increase the contact area between the primary and the secondary fluids. Breaking down the secondary stream into smaller jets facilitates more efficient the momentum exchange from the primary fluid to the secondary fluid and thereby improving the ejector  $Er$ . Furthermore, dividing the secondary fluid streams to multiple streams could distribute the secondary fluid more eventually across the primary fluid stream and enhance the mixing process. However, by increasing the secondary fluid inlet number from 3 to 4 shows no significant enhancement in ejector  $Er$  and that could be attributed to two reasons; dividing the inlet to smaller passage leads to increase the secondary flow velocity which potentially increase the shear stress at the inlet and this would impede the flow rate of the secondary fluid entering the ejector, which reduce the ejector  $Er$ . Also increasing the flow velocity could increase the turbulence within the inlet passage which lead to increased energy dissipation and hinder the entrainment of the secondary fluid and thereby the ejector  $Er$ . The second reason could due to physical limitations of the mixing chamber i.e. the available space is saturated and adding more inlets may not increase the mixing area or improve the flow distribution.

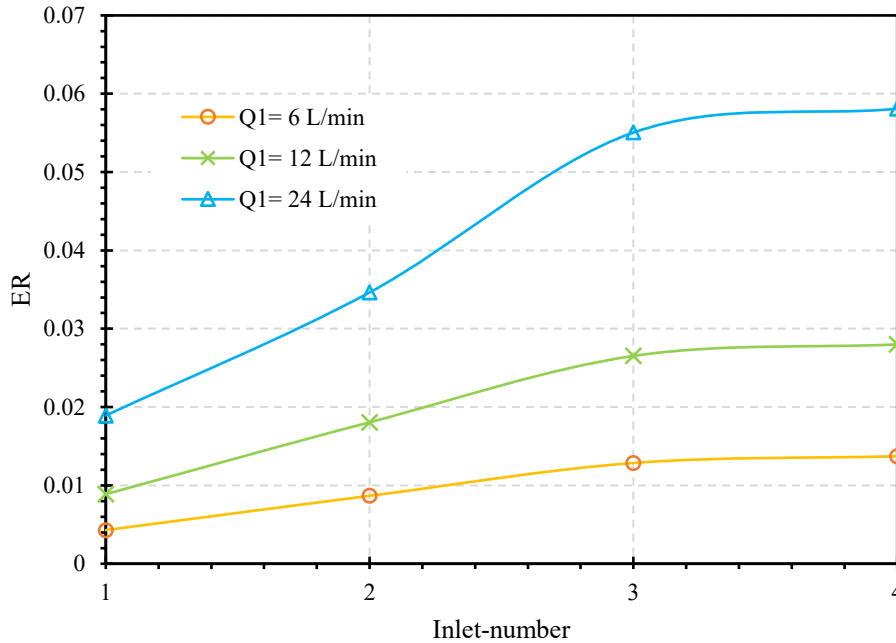


**Figure 11.** Secondary fluid inlet number vs ejector Er

The ejector velocity contour for the cases of multiple secondary inlets is shown in figure 12 for the condition of 12 L/min primary fluid and other operation and design condition are fixed and similar to that of figure 11. The velocity contour is presented in several mid planes to show the velocity at all the secondary fluid inlets of the ejector. It could be seen that the secondary fluid velocity at the inlet is increasing by the increasing of inlet number from 1 to 4 due to the decreasing of inlet passage diameter. The figure also shows that the penetration of secondary fluid in the mixing chamber is improving, that the smaller and faster jets of multiple inlets cases penetrate deeper into the primary fluid stream leading to enhance the momentum mixing between the primary and the secondary fluids. Figure 12 also shows that the secondary

fluids inlet velocity for the case of four secondary inlets center line and that could be due to the building of thicker boundary layer and thus the viscosity increasing and the frictional losses increases also, which reduce the enhancement gained by increasing the secondary fluid inlet number from 3 to 4.

The stream line for the cases of figure 12 is plotted in figure 13. It could be seen from the figure that the stream lines of secondary fluid at the secondary inlets is more complex at the multiple secondary inlet's cases compared to the single secondary inlet case. The cases of 3 and 4 secondary fluid inlet ejector show more uniform flow distribution and that could be due to well spacing of the inlets and that's make those cases have the highest ejector Er.

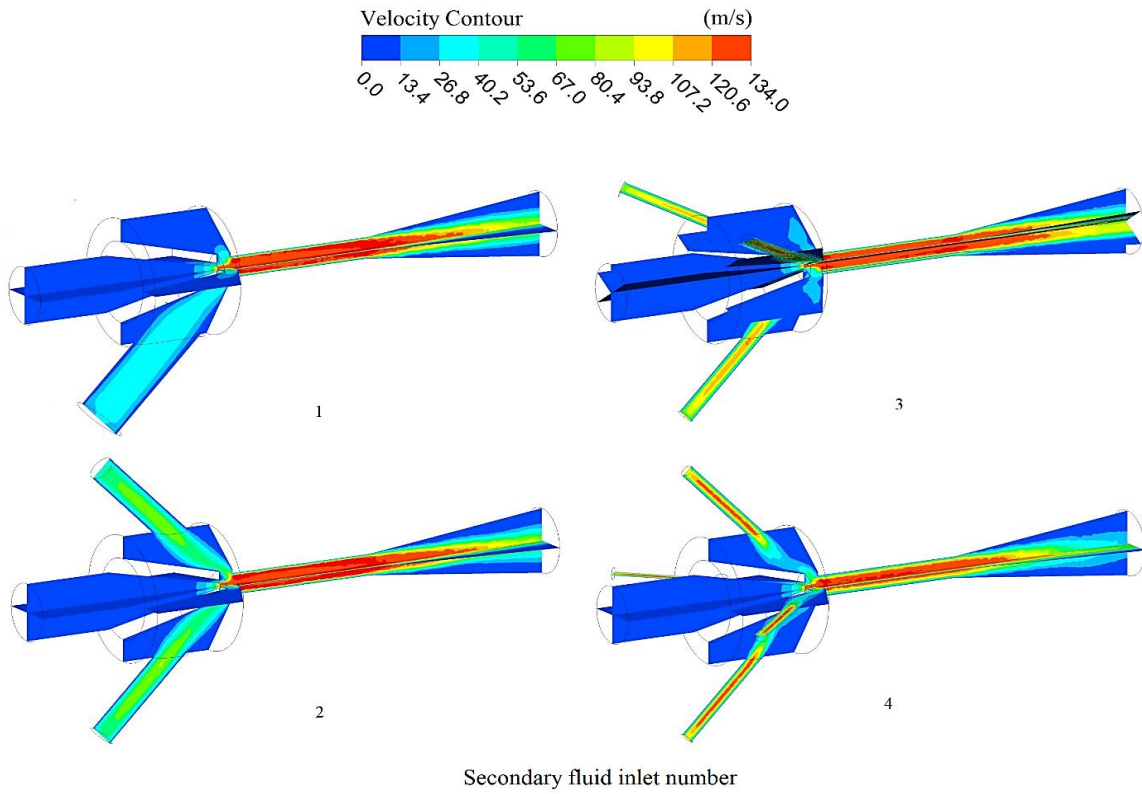


**Figure 12.** Velocity contours of the two-phase ejector at different secondary fluid inlet number and at primary fluid flow rate of 12 L/min.

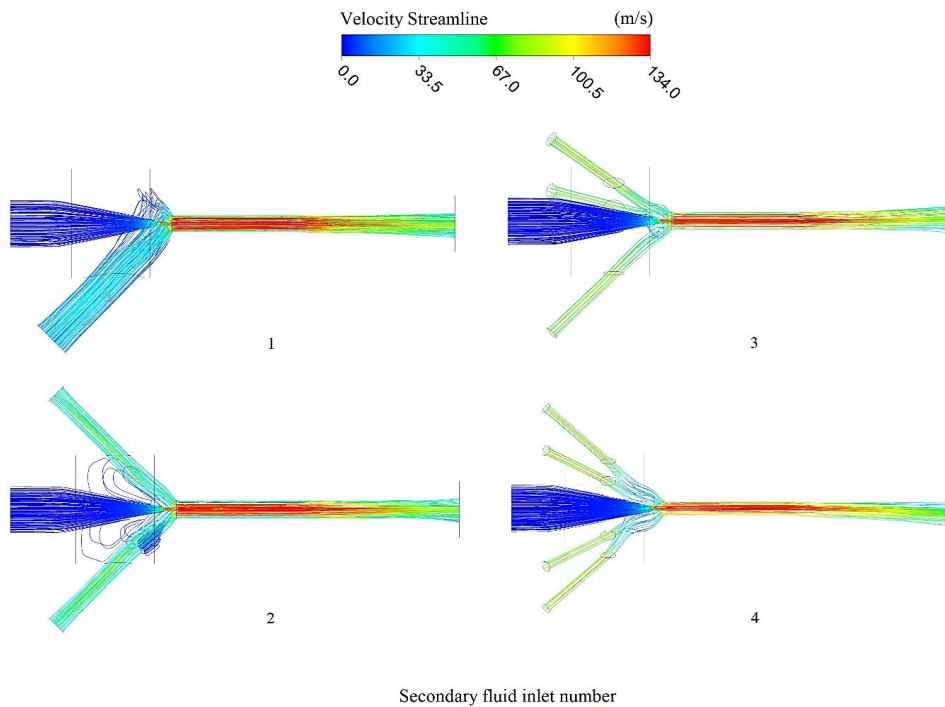


**Figure 13.** Velocity streamlines of the two-phase ejector at different secondary fluid inlet number and at primary fluid flow rate of 12 L/min.

## Conclusion

This study presents a comprehensive analysis of the influence of secondary fluid geometrical parameters on the performance of a two-phase water-steam ejector. A 3D numerical model, validated through experimental data, was employed to investigate the effects of varying secondary fluid inlet angles and the number of secondary fluid inlets across a range of primary fluid flow rates. The key findings include:

- A 45-degree secondary fluid inlet angle was determined to be optimal for maximizing ejector performance (Er). The wider angles of 60°, 75° and 90° have less ejector performance due to the reduce of the perpendicular velocity component to the primary fluid. The shallower angle of 30° has the less mixing between the primary and the secondary fluids and thereby the minimum ejector Er.
- Increasing the number of secondary fluid inlets from 1 to 3 significantly enhanced the ejector Er and that could be due to effectively increase the contact area between the primary and the secondary fluids, while further increases yielded diminishing returns due to the fact that the smaller the inlet passage has more shear stress and this would reduce the mass flow rate of the secondary fluid entering the ejector
- The effects of secondary fluid inlet parameters were more pronounced at higher primary fluid flow rates.

These results offer valuable insights for the design and optimization of two-phase ejectors, particularly in applications such as desalination. Future research could explore the impact of additional geometric parameters and operating conditions on ejector performance.

## Abbreviations

Er	entrainment ratio
<i>I</i>	turbulent intensity
<i>Re</i>	Reynold number

## Variables

<i>P</i>	pressure $N/m^2$
<i>g</i>	gravity acceleration $m/s^2$
<i>k</i>	thermal conductivity $W/m\ ^\circ C$
<i>T</i>	temperature $^\circ C$

## Greek

<i>v</i>	velocity $m/s$
$\rho$	density $kg/m^3$
$\alpha$	volume fraction (-)

## Subscript

<i>l</i>	liquid phase
<i>v</i>	vapor phase

## References

- [1] Z. Zhang, D.T. Chong, J.J. Yan, Modeling and experimental investigation on water-driven steam injector for waste heat recovery, *Appl. Therm. Eng.* 40 (2012) 189–197.
- [2] S.A. Sherif, W.E. Lear, J.M. Steadham, P.L. Hunt, J.B. Holladay, Analysis and modeling of a two-phase jet pump of a thermal management system for aerospace applications, *Int. J. Mech. Sci.* 42 (2000) 185–198.
- [3] W.X. Chen, P.B. Wei, Q.B. Zhao, D.T. Chong, J.J. Yan, Experimental study on the effect of swaying period and swaying amplitude on the dominant frequency of steam submerged jets pressure oscillation with vertically upward low mass flux, *Int. J. Heat Mass Tran.* 186 (2022), 122479.
- [4] F. Innings, L. Hamberg, Steam condensation dynamics in annular gap and multi-hole steam injectors, *Procedia Food Sci* 1 (2011) 1278–1284.
- [5] Wending Gua, Xinli Wang, Lei Wang, Xiaohong Yin, Hongbo Liu, Performance investigation of an auto-tuning area ratio ejector for MED-TVC desalination system, *Applied Thermal Engineering* 155 (2019) 470–479.
- [6] Jiapeng Liu, Lei Wang, Lei Jia, Haoyuan Xue Thermodynamic analysis of the steam ejector for desalination applications, *Applied Thermal Engineering*, 159 (2019), 113883.
- [7] N. Ruangtrakoon, T. Thongtip, S. Aphornratana, T. Sriveerakul, CFD simulation on the effect of primary nozzle geometries for a steam ejector in

- refrigeration cycle, *Int. J. Therm. Sci.* 63 (2013) 133–145.
- [8] Shakir J. Jasim, Akram W. Ezzat, Eric Hu, "Simulation and Experimental Investigation of Performance and Flow Behavior for Steam Ejector Refrigeration System", *Journal of Engineering*, Volume 29, 2023, Number 12.
- [9] Y. Zhang, X.H. Qu, G.M. Zhang, X.L. Leng, M.C. Tian, Effect of non-condensable gas on the performance of steam-water ejector in a trigeneration system for hydrogen production: an experimental and numerical study, *Int. J. Hydrogen Energy* 45 (2020) 20266–20281.
- [10] Lee Moon Soo, Lee Hoseong, Hwang Yunho, Optimization of two-phase ejector geometries using a non-equilibrium CFD model, *Appl. Therm. Eng.* 109 (2016) 272–282.
- [11] Mustafa S Mahdi, Akram W Ezzat, Eric Hu, Parametric study of low-temperature solar-assisted flash evaporation desalination systems using two-phase water–steam ejector, *Heat Transfer*, Volume 53, Issue 7, 2024, Pages 3931-3947.
- [12] M. Nakagawa, A.R. Marasigan, T. Matsukawa, A. Kurashina, Experimental investigation on the effect of mixing length on the performance of two-phase ejector for CO<sub>2</sub> refrigeration cycle with and without heat exchanger, *International Journal of Refrigeration*, Volume 34, Issue 7, 2011, Pages 1604-1613.
- [13] J. Yan, W. Cai, and Y. Li, "Geometry parameters effect for air-cooled ejector cooling systems with R134a refrigerant," *Renewable energy*, vol. 46, pp. 155-163, 2012.
- [14] Cui Li, Yanzhong Li, Lei Wang, Configuration dependence and optimization of the entrainment performance for gas–gas and gas–liquid ejectors, *Applied Thermal Engineering*, Volume 48, 2012, Pages 237-248,
- [15] Ping Zheng, Bing Li, Jingxuan Qin, CFD simulation of two-phase ejector performance influenced by different operation conditions, *Energy*, Volume 155, 2018, Pages 1129-1145,
- [16] Xuhui Wang, Sichuan Xu, Chunmei Xing, Numerical and experimental investigation on an ejector designed for an 80-kW polymer electrolyte membrane fuel cell stack, *Journal of Power Sources*, Volume 415, 2019, Pages 25-32.
- [17] Y. Han, X. Wang, H. Sun, G. Zhang, L. Guo, J. Tu, CFD simulation on the boundary layer separation in the steam ejector and its influence on the pumping performance, *Energy* 167 (2019) 469–483, <https://doi.org/10.1016/j.energy.2018.10.195>.
- [18] Akram. W. Ezzat, E. Hu, H. M. T. Al-Najjar, Z. Zhao, and X. Shu, "Investigation of steam jet flash evaporation with solar thermal collectors in water desalination systems," *Thermal science and engineering progress*, vol. 20, p. 100710, 2020.
- [19] Egoi. O. Sampedro, "A new variable mixing chamber ejector: CFD assessment," *Applied Thermal Engineering*, vol. 208, p. 118242, 2022.
- [20] J. Yan, J. Jiang, and Z. Wang, "Optimization on Secondary Flow and Auxiliary Entrainment Inlets of an Ejector by Using Three-Dimensional Numerical Study," *Entropy*, vol. 24, no. 9, p. 1241, 2022.
- [21] Yao Zhou, Jiping Liu, Yuelin Mo, Weixiong Chen, Qi Xiao, Yong Li, Junjie Yan, Numerical simulation on the direct contact condensation in a steam-water two-phase ejector with non-condensable gas, *International Journal of Thermal Sciences*, Volume 185, 2023, 108030.
- [22] Jingyang Zhang, Jinxin Geng, Sen Yang, Fengna Cheng, Guiping Zhu, Cong Wang, Zhenxi Yang, Yuanwei Lyu, Influence of geometric parameters on the performance of ejector used in aeroengine air system, *Thermal Science and Engineering Progress*, Volume 37, 2023, 101571.
- [23] Meiqi Qin, Jia Yan, Ruixin Li, Numerical study on the impact of needle and dryness fraction on two-phase ejector performance under fixed/ varied operating pressure, *Case Studies in Thermal Engineering*, Volume 61, 2024, 104976.
- [24] Omar Saeid, Gamal Hashem, Saleh Etaig, Basim Belgasim, Atul Sagade, Performance assessment of ammonia base solar ejector cooling system emphasizing ejector geometries: A detailed CFD analysis, *Energy*, Volume 301, 2024, 131770.
- [25] Xinyuan Wang, Jinbao Zheng, Zhaoyang Hao, Yage Di, Xuelong Miao, Study on the effect of pulsed gas flow on the entrainment performance of hydrogen ejector, *International Journal of Hydrogen Energy*, Volume 67, 2024, Pages 599-607
- [26] Hamid Reza Mottahedi, Saman Javadi kouchaksaraei, Mohammad Ali Faghih Aliabadi, Hesel Gharehbaei, Leyla Iraj, Sajjad Bouzari, Mohammad Akrami, Effects of motive flow temperature on holding steam ejector Performance under Condenser temperature change by considering Entropy generation and non-equilibrium condensation, *Applied Thermal Engineering*, Volume 257, Part A, 2024, 124268.
- [27] Xianying Hao, Zhiguang Chen, Xinyi Zhan, Zhicong Fang, Experimental and simulation analysis of the performance of premixed vertical ejectors, *Applied Thermal Engineering*, Volume 250, 2024, 123527.
- [28] Rashed M.Almari, Mohamed A. Abdelrahman, Mohamed A. Moawad., An experimental investigation of the Evacuated Tube solar collector in conjunction with a latent heat storage tank,

- Engineering Research Journal, Vol. 1, No. 51 Jan 2022, pp.20-28.
- [29] S. Welch and J. Wilson, "A volume-of-fluid based method for fluid flows with phase change," *Journal of Computational Physics*, vol. 160, no. 2, pp. 662–682, 2000. DOI: 10.1006/jcph.2000.6481.
- [30] ANSYS Fluent. ANSYS fluent theory guide release 2021 R2. ANSYS, Inc. July 2021
- [31] Michal Majchrzyk, Damian Dziurawicz, Michal Haida, Michal Palacz, Jakub Bodys, Rafal Fingas, Jacek Smolka, Andrzej J. Nowak, Detailed numerical investigation of the CO<sub>2</sub> two-phase ejector 3-D CFD model based on the flow visualisation experiments, *Chemical Engineering and Processing - Process Intensification*, Volume 182, 2022.
- [32] Omer Genc, Bora Timurkutluk, Serkan Toros, Performance evaluation of ejector with different secondary flow directions and geometric properties for solid oxide fuel cell applications, *Journal of Power Sources*, Volume 421, 2019, Pages 76-90.